SOILS, SEC 2 • GLOBAL CHANGE, ENVIRON RISK ASSESS, SUSTAINABLE LAND USE • RESEARCH ARTICLE

Effect of biochar amendment on PAH dissipation and indigenous degradation bacteria in contaminated soil

Liang Liu · Ping Chen · Mingxing Sun ·
Guoqing Shen · Guofeng Shang

Abstract

Purpose Biochar amendment has been extensively investigated as a method to remediate polluted soil. However, both increased and decreased pollutant biodegradation has been observed after biochar amendment is applied to soil. This study aims to demonstrate the effect of biochar amendment on 16 polycyclic aromatic hydrocarbon (PAH) dissipation and indigenous degradation bacteria in PAH-contaminated soil.

Materials and methods Four biochars derived from dairy manure and rice hull (RH) produced at pyrolysis temperatures of 350 and 500 °C were used to investigate the effect of biochar amendment on PAH dissipation in sterile and non-sterile soil. Different biochars with a rate of 4.0 % dry weight were mixed with the soil and incubated for 90 days. Sixteen PAHs in the USEPA priority-controlled list were determined by gas chromatography–mass spectrometry. Terminal restriction fragment length polymorphism and quantitative polymerase chain reaction were employed to quantify the change in the number of gene copies of the bacterial community 16S rDNA, PAH-RHDα, and nitrogen cycle genes (*nir*S).

Results and discussion The average removal efficiencies of all two-ring to four-ring PAHs in non-sterilized soil with biochar increased by 35 to 37 % compared with those in sterilized soil. Molecular biology analysis results demonstrated that biochar amendment can enhance the number of 16S rDNA, PAH-RHDα, and *nir*S gene copies in PAH-

contaminated soil. Rice hull-derived biochar pyrolyzed at 350 °C most effectively stimulated dissipation of PAHs in contaminated soil.

Conclusions The removal efficiencies of two-ring to four-ring PAHs were higher than those of five- and six-ring PAHs in actual contaminated soil amended with biochar. Biochar amendment can stimulate PAH-metabolizing bacterial activity by enhancing the number of gene copies related to PAH degradation and by changing the structure of soil microbial community. Further studies should be conducted to evaluate the effect of biochar on PAH biodegradation in different soils at different rates of biochar application.

Keywords Biochar · DNA analysis · PAHs · Soil

L. Liu · P. Chen · G. Shen (✉) · G. Shang
Key Laboratory of Urban Agriculture (South), Ministry of Agriculture, School of Agriculture and Biology, Shanghai Jiao Tong University, Shanghai 200240, People's Republic of China
e-mail: gqsh@sjtu.edu.cn

M. Sun
Shanghai Entry–Exit Inspection and Quarantine Bureau, Shanghai 200135, People's Republic of China

1 Introduction

Polycyclic aromatic hydrocarbon (PAH) is a class of organic compounds consisting of two or more fused benzene rings. PAH-contaminated soil is a serious environmental concern because PAHs are highly toxic and mutagenic (Haritash and Kaushik 2009). The United States Environmental Protection Agency (US-EPA) and the European Union listed 16 PAHs as priority pollutants (Keith and Telliard 1979; European Union, Commission Recommendation 2005). Bioremediation is considered as an environmentally friendly technology to abate soil contamination. However, the extensive practice of bioremediation in the field is limited by low efficiency and long-term maintenance (Qin et al. 2013).

Biochar is produced by the thermal decomposition of biomass under oxygen-limited conditions (pyrolysis). Investigations have demonstrated beneficial effects of biochar on soil microbial activity, soil fertility, nutrient availability, and reduction of greenhouse gas emissions (Steinbeiss et al. 2009; Jeffery et al. 2013). Studies have also been conducted to

investigate the feasibility of using biochar to accelerate the degradation of PAHs in soil (Chen et al. 2012). Quilliam et al. (2013) considered that biochar can facilitate the degradation of naturally occurring PAHs. Vasilyeva et al. (2010) found that adding activated carbon (AC) helps microorganisms overcome the toxicity of polychlorinated biphenyls. Hale et al. (2011) also reported that biochar amendment elicits a stimulatory effect on PAH biodegradation in soil. Biochar application can be cheaper than other remediation techniques because waste source materials are essentially free, and biochar production requires less energy and entails lower costs (Hale et al. 2011). However, Rhodes et al. (2008) reported that black carbon strongly sorbs phenanthrene, causing reductions in extractability and bioaccessibility to degrading microorganisms to a lesser extent than other substances. Karapanagioti et al. (2001) showed that slow sorption kinetics limits spiked phenanthrene biodegradation in sediment slurries containing coal particles. Nevertheless, Colombo et al. (2011) emphasized that studies using single PAH do not show the complexity of PAH degradation in natural environment. When present in mixtures, PAHs can influence the rate and extent of biodegradation of other mixture components. In some cases, these interactions may be positive, resulting in an increase in biodegradation of one or more components; in other cases, negative effects have been observed (Dean-Ross et al. 2002). With these antagonistic outcomes, the effect of biochar amendment on PAH dissipation cannot be readily anticipated. A potential concern regarding the application of strong sorbents at contaminated sites is the impact on the intrinsic biodegradation of organic pollutants (Rhodes et al. 2008). Therefore, the effect of biochar on intrinsic microbial pollutant degradation should be investigated, particularly at sites polluted with PAH mixture.

Many microorganisms are adapted to metabolize PAHs under aerobic conditions. Ring-hydroxylating dioxygenases (RHD) are multicomponent bacterial enzymes that catalyze the first step in the oxidative degradation of PAHs (Cerniglia 1993). The genes encoding the catalytic domain of PAH-RHDα (α-subunit) have been extensively used as biomarkers of a PAH-degrading potential in different environments; as such, this subunit is considered as an important tool used to study RHD biodiversity (Jurelevicius et al. 2012). A positive correlation was also observed between the relative abundance of the genes involved in bioremediation and the potential for contaminant degradation (Schneegurt and Kulpa 1998). In addition, anaerobic microorganisms can use nitrate and/or nitrite as electron acceptors to degrade various PAHs (Meckenstock et al. 2004). Ambrosoli et al. (2005) illustrated that anaerobic PAH degradation occurs in soil with a mixed bacterial consortium under denitrifying conditions. Nitrite reductase is the main enzyme in the denitrification pathway (Ye et al. 1994). Nitrite reductase has two primary forms: one form contains cytochromes c and $d1$ (cd1-NiR) and the other

form contains two copper centers (Cu-NiR) at each active site. The enzyme Cu-NiR is encoded by the *nir*K gene, and cd1-NiR is encoded by the *nir*S gene. Despite their structural differences (Williams et al. 1997), the two forms of nitrite reductase exhibit the same physiological function in denitrifying bacteria. Guo et al. (2011) reported a positive correlation between potential denitrification activity and copy number of denitrifying functional genes; furthermore, denitrifiers harboring the *nir*S gene are more sensitive than those harboring other genes. To date, limited information is available regarding the effect of biochar on denitrifying bacteria during PAHs biodegradation (Guo et al. 2011).

Studies have demonstrated the complex effects of biochar on PAH removal from soil. These effects can be related to certain factors, including the origin and production method of biochar and microbial properties (Qin et al. 2013). The net ability of biochar to enhance soil properties depends partly on specific qualities of biochar and site condition. Biochar is heterogeneous, not single material, because different nutrient contents and chemical structures lead to the lack of a "one-size-fits-all" biochar (Spokas et al. 2012). We hypothesized that biochar amendment can stimulate dissipation of PAHs by enhancing the activity of the bacteria known to metabolize PAHs in contaminated soil. The relative magnitude of response possibly depends on the specific properties of biochar and individual PAHs. This study primarily aimed to (1) compare the removal efficiencies of PAHs in soil with biochar and to (2) determine whether or not biochar amendment can activate the indigenous microbial degradation of PAHs. To accomplish these objectives, we used biochars derived from dairy manure (DM) and rice hull (RH) produced at pyrolysis temperatures of 350 and 500 °C. These biochars were then utilized to investigate the effect of biochar amendment on PAH dissipation in sterile and non-sterile soil. Terminal restriction fragment length polymorphism (T-RFLP) and quantitative polymerase chain reaction (qPCR) were also employed to quantify the change in the number of gene copies of 16S rDNA, PAH-RHDα, and nitrogen cycle genes (*nir*S) of the bacterial community.

2 Materials and methods

2.1 Preparation of biochar

The biochar used in this study was produced from RH and DM biomass by a typical slow pyrolysis process. In a typical procedure, air-dried RH and DM were placed in a stainless steel reactor and heated in a muffle furnace (Thermo Fisher Scientific, Inc., Pittsburgh, PA, USA) under O$_2$-limited condition at 350 and 500 °C. Temperature was increased to the selected values at a speed of 25 °C min^{-1} and held for 4 h. After 4 h of heating, the sample was allowed to cool to room

temperature. Different biochars were sieved using a 1-mm sieve and characterized for Fourier transform-infrared (FTIR), mineral composition, and elemental concentrations (Fig. 1 and Table 1). The pH of biochars was determined in a mixture of 5 g of biochar and 10 mL of deionized water after 1 h of equilibrium was maintained. Ash content was measured by heating the biochars at 1,000 °C for 2 h and calculated using the following equation: Ash (%)=(B1/B2)×100, where B1 and B2 are the weights of biochar after and before heating, respectively. Carbon and nitrogen contents were determined using elemental analysis–stable isotope ratio mass spectrometer. Specific surface area (SSA) was detected by nitrogen adsorption isotherms at 77 K by using a surface area and porosimetry analyzer.

2.2 Soil and microcosm preparation

The soil used in this study is a historically contaminated soil (paddy soil) collected from a coking plant at Longwu Road Minhang in Shanghai, China (31° 4′ 44.66″ N, 121° 27′ 37.54″ E), which was founded in 1958. Soil physical and chemical properties and PAH concentration are shown in Table 2. Three soil cores were obtained within a 1-m radius of the sampling site and analyzed as composite samples. In particular, soil samples at a depth of 0 cm to 20 cm were collected, air dried, passed through a 2-mm sieve, and stored at 4 °C until use.

The soil was subjected to different treatments for 90 days. For each treatment with three independent replicates, 1-L plastic containers (13 cm in diameter and 10 cm in height) were prepared as microcosms, each containing 1 kg of soil. Three different trials were performed in triplicate: (A) sterilized and non-sterilized soil without biochar as control

samples, (B) non-sterilized soil amended with 4 % (w/w) biochar, and (C) steam-sterilized soil amended with 4 % (w/w) biochar. In all of the treatments, water content was adjusted to 60 % of water holding capacity. Soil water content was restored once a week by controlling the weight. Mesocosms were covered with perforated parafilm and incubated at 25 °C inside an incubation cabinet. After the expected period, soil samples were collected and stored at 4 °C until analysis of PAHs, bacterial community, and qPCR. pH and organic matter (OM) content, C, N, and ash in biochar were determined by standard methods (ASTM 2000; Miller and Keeney 1982; US-EPA 1986). PAHs were analyzed by gas chromatography–mass spectrometry (GC–MS; Agilent7890A/5975, USA) according to EPA method 8270.

2.3 Sample analysis by GC–MS

Soil samples were extracted with dichloromethane and acetone (1:1) by accelerated solvent extraction. The extracts were evaporated to 1 mL by using a rotary evaporator and purified using silica chromatography columns. The final concentrated extracts were analyzed using an Agilent (USA) 7890 GC on a DB-5 MS capillary column (J&W Scientific, USA) coupled with 5975 MSD. A silica fused capillary column was used, in which helium was used as a carrier gas at a constant flow rate of 1 mL min^{-1}. The GC oven temperature was programmed to ramp from 50 to 200 °C at 10 °C min^{-1} to 300 °C at 10 °C min^{-1}. Temperature was kept constant at 300 °C for 8 min. Injector and detector temperatures were 280 and 300 °C, respectively. Mass spectra were obtained at an electron ionization mode, and selected ion monitoring mode was performed using the molecular ions selective for individual PAHs. The recoveries of deuterated surrogated PAHs from

Fig. 1 Fourier transform-infrared spectra of biochars. *DM* dairy manure-derived biochar; *RH* rice hull-derived biochar; 350 and 500 °C, pyrolysis temperatures
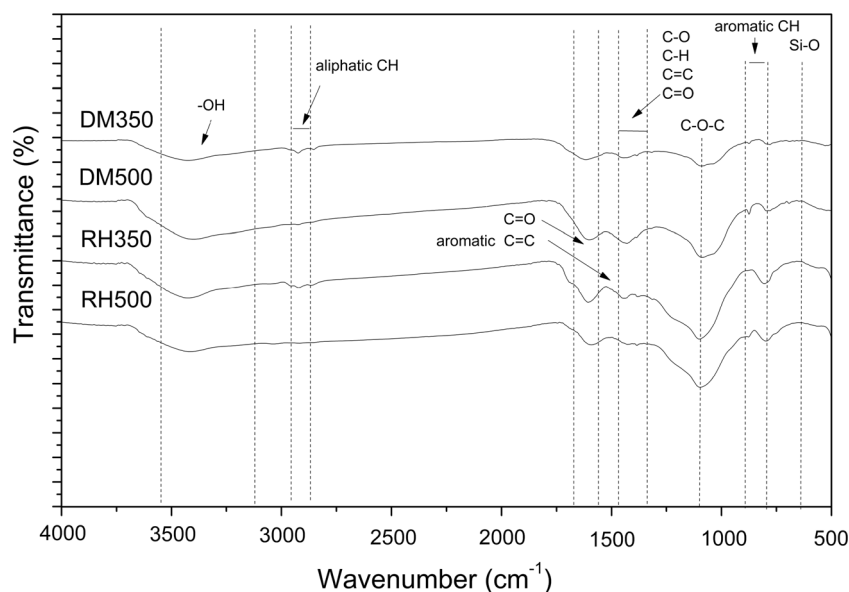
Table 1 Selected properties of the biochars

Biochar	$\sum$PAHs (mg kg^{-1})	Yield (%)	SSA (m^2 g^{-1})	TPV (cm^3 g^{-1})	Ash (%)	pH	C (%)	N (%)	C/N
DM350	0.05±0.03	38.67	5.61	0.075	32.88	9.72±0.01	42.85±0.02	2.36±0.03	18.16
DM500	0.23±0.02	34.63	21.94	0.028	52.55	10.20±0.02	44.67±0.01	1.98±0.04	22.56
RH350	0.02±0.01	48.63	27.80	0.055	30.64	9.55±0.01	37.32±0.04	0.47±0.08	79.40
RH500	0.45±0.01	32.67	71.32	0.051	51.27	11.06±0.04	40.22±0.02	1.23±0.04	32.70

All values represent means±SD

DM dairy manure-derived biochar, *RH* rice hull-derived biochar, *350 and 500* pyrolysis temperatures (°C), *SSA* specific surface area, *TPV* total pore volume

soil were checked in accordance with surrogate PAH-deuterated standards (acenaphthene d$_{10}$, chrysene d$_{12}$, naphthalene d$_8$, perylene d$_{12}$, and phenanthrene d$_{10}$). The results showed satisfactory recovery, in which average recovery ranged from 82.3±9.2 % to 95.2±7.6 %. Procedure blanks and parallel samples were analyzed simultaneously.

2.4 Real-time PCR analysis

Total DNA was extracted from the soil samples by using E.Z.N.A. soil DNA kit (Omega BioTek, Inc., Norcross, GA, USA) according to the manufacturer's instructions. 16S rDNA, PAH-RHDα, and *nir*S genes of the soil samples were assessed by real-time PCR in an ABI StepOne Plus system (Applied Biosystems, USA). Primers and amplification protocols were specifically described by Meng and Zhu (2010). The PCR mixture (20 μL of final volume) contained 2 μL of template DNA (with filtered sterile molecular biology water as a negative control; Sigma-Aldrich), 10 μL of SYBR Premix Ex *Taq* II (2×; TaKaRa, DaLian), 0.4 μL of ROX reference dye (50×), and 10 μmol of each primer. The following two-stage temperature profile was used for amplification: heating at 95 °C for 30 s, followed by 40 cycles of denaturation at 95 °C for 5 s and primer annealing at specific annealing temperatures [55 °C for 30 s for 16 s rDNA and Gram-positive (GP) gene, 58 °C for 30 s for Gram-negative (GN) gene, and 60 °C for 30 s for *nir*S gene]. At the end of real-time PCR, a melting curve was drawn. Green signal intensities were obtained from 60 to 95 °C at an increasing rate of 0.4 °C per 10 s. The corresponding plot of change in fluorescence versus temperature showed a single peak for each amplicon at specific melting temperature.

2.5 Standard curve

For each set of primers, a standard curve was obtained from the standard DNA prepared from pMD18-T plasmids (TaKaRa, DaLian) containing the cloned target sequences. The obtained sequences were aligned against known sequences with BLASTN. The result showed that the amplified

sequence contained the correct length and was closely related to the desired sequence. The plasmid DNA concentration was quantified using a Nano-Drop 2000 spectrophotometer (Nano-Drop Technologies, Wilmington, DE, USA). The copy number of the genes per microliter of plasmid solution was calculated based on the following equation: copy number of

Table 2 Soil physical and chemical properties and PAH concentration

Characteristic		Value
pH		7.35±0.01
OM (g kg^{-1})		16.17±0.05
N (g kg^{-1})		1.15±0.02
P (g kg^{-1})		1.36±0.22
CEC (cmol kg^{-1})		15.60±0.68
Particle size distribution (mm)	Sand (0.01–1.0)	51.49±0.02
	Silt (0.001–0.01)	28.37±0.02
	Clay (<0.001)	20.14±0.03
PAH		Concentration (mg kg^{-1} dry soil)
Naphthalene		0.03±0.03
Acenaphthylene		0.03±0.02
Acenaphthene		0.08±0.03
Fluorene		0.12±0.03
Phenanthrene		0.30±0.01
Anthracene		0.27±0.03
Fluoranthene		0.69±0.05
Pyrene		0.56±0.03
Benzo[*a*]anthracene		0.39±0.07
Chrysene		0.46±0.08
Benzo[*b*]fluoranthene		0.39±0.03
Benzo[*k*]fluoranthene		0.41±0.02
Benzo[*a*]pyrene		0.63±0.02
Dibenz[*a,h*]anthracene		0.22±0.03
Benzo[*g,h,i*]perylene		0.15±0.05
Indeno[1,2,3-*cd*]pyrene		0.22±0.01
Total		4.91±0.53

All values represent means±SD

OM organic matter, *CEC* cation exchange capacity

the genes [$\mu L = (L \times C)/(N \times M \times 10^9)$], where M is the molecular weight of an average base pair of DNA (660 g mol^{-1}), L is Avogadro's constant (6.02×10^{23} mol^{-1}), N is the length of the template containing the gene fragment and PMD-18T vector, and C is the mass concentration of plasmid in nanograms per liter, which was measured using a Nano-Drop 2000 spectrophotometer. Stock solutions of standard DNA were prepared at a concentration of 10^9 copies of plasmid per microliter. For the calibration curves, DNA standards ranging from 10^9 to 10^2 target gene copies per microliter were prepared by diluting the stock solutions. All of the standard curves were linear ($R^2 > 0.99$) and eight orders of magnitude (10^9 to 10^2 μL^{-1}) higher than the number of gene copies. Each sample was run in triplicate, and each experiment was repeated at least twice. In each run, the accuracy of target gene detection in the soil samples was confirmed by comparing the melting curves and agarose analysis results of qPCR products with those obtained from DNA extracted from model organisms (positive control) to avoid false detection in the environmental samples.

2.6 T-RFLP analysis of the PAH-RHDα gene

The heterogeneity of the PAH-RHDα gene sequences from the DNA samples of control and biochar-amended PAH-contaminated soils were analyzed by T-RFLP. The soil DNA pellet was dissolved in 60 μL of TE buffer (pH 8.0). The recovered DNA was further purified using an AxyPrep^{TM} gel extraction kit (AxyGen Hangzhou, P. R. China). The extracted purified DNA was visualized by electrophoresis in 1 % agarose gels and spectrophotometrically quantified by Nano-Drop 2000. The extracted DNA was then diluted to 10 ng mL^{-1} before PCR amplification was performed. The fragment of the bacterial PAH-RHDα (GP, 292 bp) gene was amplified by PCR using the primers labeled with 6-carboxyfluorescein at the 5′-end. PCR amplification was performed under the following conditions: an initial denaturation step of 95 °C for 180 s, followed by 25 cycles of denaturation at 94 °C for 45 s, annealing at 52 °C for 30 s, and elongation at 72 °C for 180 s. Cycling was completed with a final elongation step of 72 °C for 10 min. PCR products were purified using an AxyGen gel extraction kit. DNA was then resuspended in nuclease-free double-distilled water and spectrophotometrically quantified by Nano-Drop 2000. Approximately 2 mg of aliquots of each pooled PCR product was digested for 16 h at 37 °C with MspI (Fermentas International Inc., Shenzhen, China). The size of individual terminal fragments (T-RFs) was determined with an ABI Prism 3130 genetic analyzer (Applied Biosystems, Foster City, CA, USA). The peaks in each profile were related to specific fragment lengths based on a size marker (500 MapMarker). Raw T-RFLP data were retrieved using Peak Scanner v1.0 (Applied Biosystems,

Foster City, CA, USA). The size (in base pairs) of each peak (T-RF) was used to indicate an operational taxonomic unit (OTU); the areas of the peak were used to determine relative abundance in the profile. T-RF sizes were then aligned to the nearest size. In each sample, T-RF areas were normalized by the total area of T-RFs in that sample.

2.7 Statistical analysis

All of the results were expressed as the mean of three replicates per sample and standard deviation. One-way ANOVA for independent samples was performed using SPSS 12.0 (SPSS Inc., Chicago, IL) with significance defined at $P < 0.05$, unless otherwise stated. Multiple comparisons of significant differences were conducted using Duncan's test ($P < 0.05$). PAH removal efficiency was calculated using the following formula: PAH removal efficiency (%)$=(P_0 - P_B) \times 100/P_0$, where P_0 and P_B denote the concentrations of PAHs in soil with and without biochar, respectively.

3 Results and discussion

3.1 Characterization of biochar

Table 1 shows the properties of the biochars derived from DM and RH at pyrolysis temperatures of 350 and 500 °C. The ash contents of the biochars at 500 °C were higher than those at 350 °C (32.88 % for DM350, 30.64 % for RH350, 52.55 % for DM500, and 51.27 % for RH500). As pyrolysis temperature increased, amorphous carbon was burnt, producing carbon dioxide (Baldock and Smernik 2002); thus, high ash content was obtained. In addition, the ash contents of biochars derived from DM were higher than those of biochars derived from RH (Brewer et al. 2009). The carbon content at 350 °C was lower than that at 500 °C. Biochars derived from DM contained higher nitrogen than those from RH. This result is in agreement with an earlier study on biochars with nitrogen contents (Cantrell and Martin 2012). All of the biochars were alkaline, but the biochar at 500 °C exhibited a higher pH than that at 350 °C. In general, biochars with high mineral ash content show greater pH values than those with low ash contents.

For all biochars, pH increases as pyrolysis temperature increases. The mechanism of a decrease in pH involves the oxidation of C to form acidic carboxyl groups (Cheng et al. 2006). An increase in pH is likely related to the dissolution of alkaline minerals (Lehmann et al. 2011).

Table 1 also shows that the C/N ratio of DM and RH biochars varied between 22.56 and 79.40. RH350 exhibited the highest C/N ratio (79.40) among these biochars. Steinbeiss et al. (2009) reported that biochar obtained from different

sources determines the significant changes in microbial community composition. For instance, biochar with very low C/N ratio favors fungi, whereas biochar obtained from glucose (without N) promotes GN bacteria.

The FTIR spectra of DM and RH biochar (Fig. 1) indicated that the four biochars contain C=C and C=O stretching in the aromatic ring at 1,620 cm^{-1}. The FTIR results differed in biochars derived at different temperatures (Fig. 1). Aromatic CH increased the height of peaks at 755 to 800 cm^{-1} in RH500 and DM500. The intensity of C–O (1,436 to 1,490 cm^{-1}) and C–H groups (1,426 to 1,385 cm^{-1}) decreased as temperature was increased to 500 °C. The amount of aromatic C=C increased in DM500, as indicated by the increasing height of peaks at 1,580 to 1,462 cm^{-1}, but this result was not observed in RH500. The amount of C=O units decreased, as indicated by the decreasing peaks at 1,650 to 1,690 cm^{-1}. Hydroxyl was oxidized as indicated by the loss of peak intensity at 3,200 to 3,664 cm^{-1} at a high pyrolysis temperature (500 °C). As heating temperature increased (500 °C), aliphatic carbon was transformed to aromatic carbon, as indicated by the reduction in intensity of peaks at 2,886 to 2,848 cm^{-1}.

3.2 Removal of PAHs in contaminated soil amended with biochar

Figure 2 and Table 3 show the removal of 16 PAHs in actual contaminated soil amended with biochar. The results showed that the removal efficiencies of two-ring to four-ring PAH were higher than those of five- and six-ring PAH. The greatest dissipation was observed in RH350. DM350 also dissipated benzo[b]fluoranthene, benzo[k]fluoranthene, and benzo[a]pyrene. The removal efficiencies of these substances were 5.13, 7.32, and

4.76 %, respectively. However, the amount of five- and six-ring PAHs slightly increased in soil with RH500 and DM500 produced at high pyrolysis temperature. This finding may be attributed to the native PAHs in the biochar and the recalcitrant effect of five- and six-ring PAHs on soil-degrading bacteria (Hilber et al. 2012). A previous study also showed that five- and six-ring PAHs exhibit only <10 % dissipation even after 24 weeks. Keiluweit et al. (2012) demonstrated that the total yield and composition of PAHs in biochars are strongly dependent on feedstock and pyrolysis temperature. At >500 °C, PAHs form larger aromatic structures via a free radical pathway followed by pyrosynthesis.

The results obtained from sterilized and non-sterilized soil with biochar were compared with those obtained from sterilized soil without biochar to differentiate the roles of biotic versus abiotic processes in the enhanced rate of PAHs dissipation in the presence of biochar. The average removal efficiencies of two-ring to four-ring PAHs in non-sterilized soil with DM and RH increased by 35 and 37 % as against those in sterilized soil, respectively. These results demonstrated that biochar amendment activated the indigenous microbial degradation of two-ring to four-ring PAHs. We assume that a high amount of metabolites can be absorbed onto the biochar, thereby leading to a significant reduction in soil toxicity and biodegradation enhancement (Qin et al. 2013). In addition, many microorganisms show chemotaxis toward PAHs, and this mechanism leads to increased degradation by reducing the distance between the microorganism and the contaminant caused by PAH absorption; this factor is often the major obstacle for dissipation (Fredslund et al. 2008; Peng et al. 2008).

Fig. 2 Total removal efficiency of PAHs in sterilized and non-sterilized soil with biochar. *DM* dairy manure-derived biochar; *RH* rice hull-derived biochar; 350 and 500 °C, pyrolysis temperatures

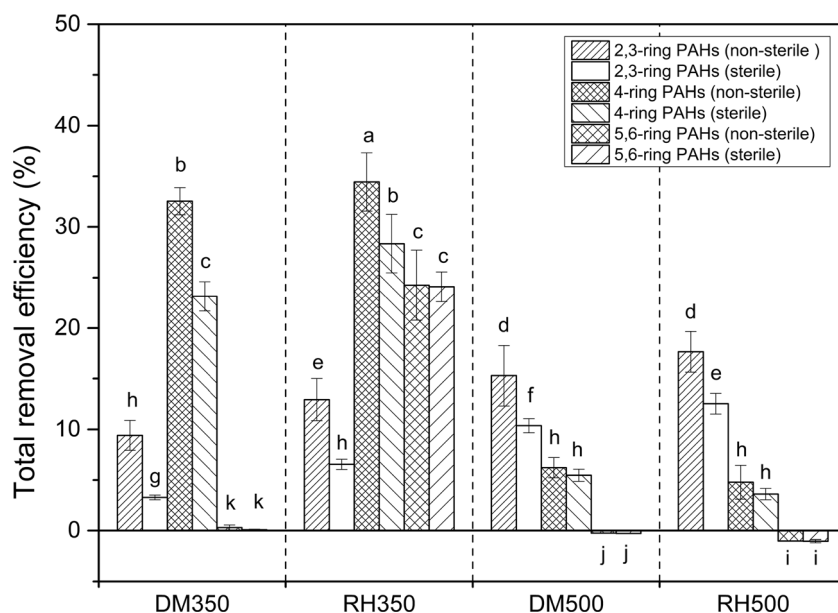**Table 3** The removal efficiencies of different PAHs

PAHs	Dairy manure				Rice husk			
	350 °C		500 °C		350 °C		500 °C	
	Non-sterile	Sterile	Non-sterile	Sterile	Non-sterile	Sterile	Non-sterile	Sterile
Naphthalene	*	*	33.33±4.56	26.67±2.56	*	*	*	*
Acenaphthylene	*	*	*	*	*	*	33.33±4.33	23.33±2.33
Acenaphthene	33.33±2.69	16.67±0.69	66.67±8.84	38.28±3.84	13.33±0.36	7.28±0.36	86.67±6.31	53.33±6.31
Fluorene	*	*	7.69±3.82	6.69±0.82	7.69±1.48	5.89±0.48	15.38±7.22	13.38±1.22
Phenanthrene	20.67±2.53	12.36±2.53	13.33±5.28	10.67±1.28	30.34±4.23	18.67±1.13	13.33±1.57	11.22±1.57
Anthracene	11.11±2.34	8.96±1.34	3.70±1.33	3.41±0.33	22.22±3.45	18.34±1.45	3.70±1.35	3.50±0.35
Fluoranthene	23.19±3.47	15.37±3.47	7.25±4.58	6.69±2.58	36.23±2.18	26.15±2.18	7.25±3.88	7.67±0.88
Pyrene	23.21±3.33	18.29±2.54	5.36±2.37	5.32±0.37	33.93±5.88	28.82±1.41	7.14±2.67	6.78±0.67
Benzo[a]anthracene	17.95±2.83	12.37±1.83	7.69±3.60	6.96±1.60	35.89±3.44	28.35±1.25	2.56±1.32	2.42±0.35
Chrysene	71.74±3.27	67.88±5.27	6.52±0.35	5.52±0.35	32.60±2.49	20.61±2.43	2.17±1.28	2.01±0.27
Benzo[b]fluoranthene	5.13±2.31	5.13±1.31	−2.56±0.15	−2.73±0.15	28.21±5.38	26.21±1.65	−10.26±3.35	−10.55±2.35
Benzo[k]fluoranthene	7.32±0.91	7.23±1.52	−2.44±1.22	−2.48±0.24	29.26±6.43	25.37±3.43	−9.76±2.44	−9.69±2.44
Benzo[a]pyrene	4.76±0.32	4.67±1.32	−3.17±1.53	−3.22±1.43	28.57±8.52	30.22±1.62	−14.29±4.88	−14.67±1.88
Dibenz[a,h]anthracene	−4.23±1.02	−4.35±0.65	*	*	24.65±7.35	20.33±4.35	−20.33±5.25	−22.25±2.34
Benzo[g,h,i]perylene	−5.88±3.44	−6.03±0.44	*	*	23.53±4.68	22.37±5.68	−11.76±2.23	−12.09±2.23
Indeno[1,2,3-cd]pyrene	−8.42±2.25	−10.03±2.25	−4.21±1.74	−5.01±0.72	24.37±2.87	22.86±3.27	−32.67±5.51	−32.37±2.51

* Means not detected

3.3 Quantification of the 16S rDNA gene

The 16S rDNA gene copy numbers were measured by qPCR to further explore the biochar-mediated stimulation of PAH-degrading population. Figure 3 shows that the copy number of the 16S rDNA gene of bacteria in the treatment ranged from 3.25×10^8 to 5.06×10^8 copies g^{-1} dry soil. Bacteria were more abundant in the soil with biochar than in the soil without biochar. The sorption of PAHs and the pH changes in soil

may play a major role (Lehmann et al. 2011). The gene copies in all of the treatments were higher in biochar at 350 °C than in biochar at 500 °C. The maximum total number of 16S rDNA gene copies was 5.06×10^8 copies g^{-1} dry soil in the soil with RH350. No significant difference was observed in the gene copy between DM500 (4.10×10^8 copies g^{-1} dry soil) and RH500 (4.14×10^8 copies g^{-1} dry soil). These results indicated that low-pyrolysis temperature biochar, particularly RH350, was more conducive to microbial growth in PAH-
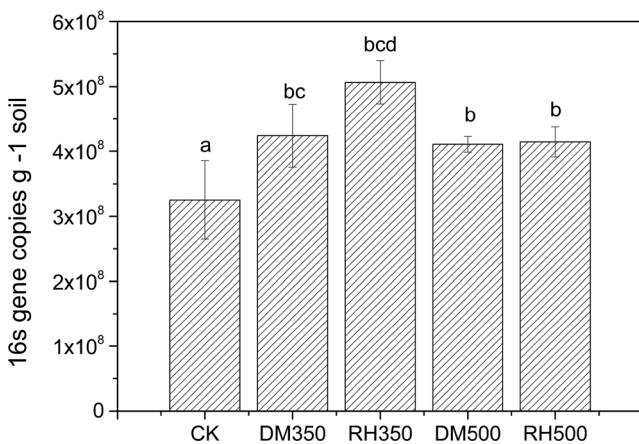
Fig. 3 Copy number of the 16S gene. Data are means±SE; n=3. Different *letters* indicate significant differences (P<0.05) between treatments. *CK* the non-sterilized soil without biochar; *DM* dairy manure-derived biochar; *RH* rice hull-derived biochar; 350 and 500 °C, pyrolysis temperatures
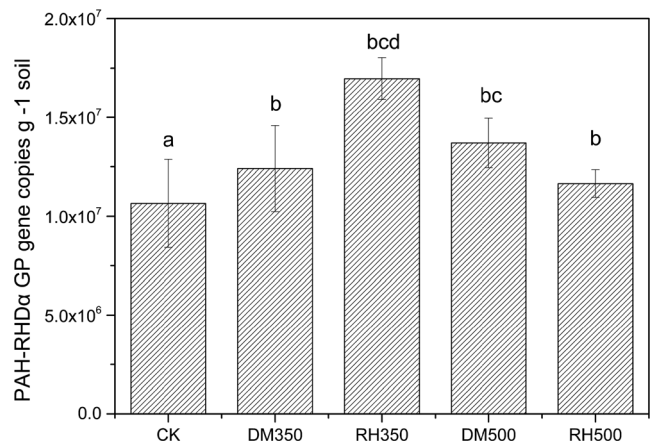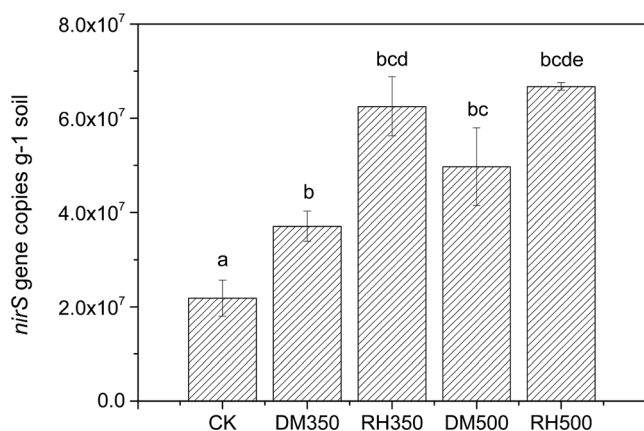
Fig. 4 Copy number of the PAH-degrading population (PAH-RHDα) GP gene. Data are means±SE; n=3. Different *letters* indicate significant differences (P<0.05) between treatments. *CK* the non-sterilized soil without biochar; *DM* dairy manure-derived biochar; *RH* rice hull-derived biochar; 350 and 500 °C, pyrolysis temperatures

Fig. 5 Copy number of the *nir*S gene. Data are means±SE; *n*=3. Different *letters* indicate significant differences (*P*<0.05) between treatments. *CK* the non-sterilized soil without biochar; *DM* dairy manure-derived biochar; *RH* rice hull-derived biochar; 350 and 500 °C, pyrolysis temperatures

contaminated soil than high-pyrolysis temperature biochar. These results may be related to the C/N ratio and pH in biochar (Hgberg et al. 2007; Wang et al. 2012). In addition, several authors suggested that a porous structure, together with its ability to absorb soluble organic matter, gases, and inorganic nutrients, likely provides a highly suitable habitat for microbes to colonize (Pietikäinen et al. 2000).

3.4 Quantification of the PAH-RHDα gene

Cébron et al. (2008) designed a PAH-RHDα-GP primer set against the genes (*nar*Aa, *phd*A/*pdo*A2, *nid*A/*pdo*A1, and *nid*A3/*fad*A1) common to the GP PAH degraders. All of these genes are related to the degradation of two-ring to four-ring PAHs, such as naphthalene, phenanthrene, pyrene,

anthracene, fluoranthene, and benzo[*a*]pyrene (Moody et al. 2001). Therefore, this PAH-RHDα primer set was selected to investigate the biochar amendment of indigenous PAH-degrading bacteria in contaminated soil. Figure 4 shows a significant increase in the copy number of the PAH-RHDα GP gene after biochar was added compared with the control sample (1.06×10^7 copies g^{-1} dry soil). As expected, the maximum gene copies were found in the soil with RH350 (1.73×10^7 copies g^{-1} dry soil). These results correspond to the finding that two-, three-, and four-ring PAHs significantly dissipated in the soil with DM and RH biochars, particularly in RH350. Therefore, the tested biochar may significantly stimulate the growth of PAH-degrading bacterial population carrying such genes. Numerous bacteria can degrade low molecular weight (LMW) PAHs; high molecular weight PAHs are more recalcitrant, and relatively few microorganisms can use these substances as a carbon source (Cébron et al. 2009). The genes that encode the enzymes involved in different metabolic steps of aerobic bacterial PAH-degradation pathways have been described in a wide range of GN bacterial and GP bacterial strains (Habe and Omori 2003). However, the PAH-RHDα GN genes were not detected in control and treatments in this study. GP PAH degraders may be considered as the microorganisms dominating PAH-polluted soil (Uyttebroek et al. 2006).

3.5 Quantification of the *nir*S gene

Figure 5 shows the effect of biochar amendment on the copy number of the *nir*S gene. The copy numbers in the soil with four biochars were significantly higher in the *nir*S gene (3.71×10^7 to 6.45×10^7 copies g^{-1} dry soil) than in the control gene (2.19×10^7 copies g^{-1} dry soil). The *nir*S gene copies in

Fig. 6 Community structure of Gram-positive (GP) PAH degradation bacteria. The relative abundance of T-RF used as the measurement of composition of bacterial community is also shown; data are means±SE; *n*=3
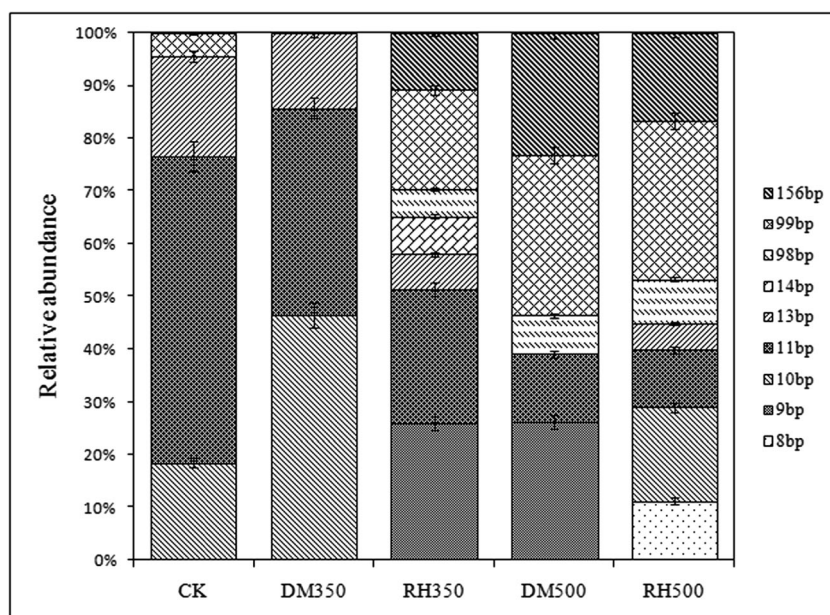
the soil amended with biochar at 500 °C (4.96×10^7 and 6.48×10^7 copies g^{-1} dry soil for DM500 and RH500, respectively) were higher than those in the soil with biochar derived at low temperature (3.71×10^7 copies g^{-1} dry soil in DM350 and 6.23×10^7 copies g^{-1} dry soil in RH350) in the PAH-contaminated soil. These results showed that the tested biochar significantly enhanced the copy number of the *nir*S gene and stimulated denitrifier growth. Studies have demonstrated that LMW PAHs can be biodegradated under denitrifying conditions (Lu et al. 2012). Therefore, enhancement of the two-ring to four-ring PAH dissipation and biodegradation by biochar amendment may also be attributed to the increase in anaerobic degradation of PAHs.

3.6 Structure of PAH degradation microbial community

To further understand the microbial PAH degradation processes in soil with biochar, we performed the T-RFLP fingerprint assay based on the specific homologous genes that encode the PAH-RHDα from GN (*Pseudomonas*, *Ralstonia*, *Comamonas*, *Burkholderia*, *Sphingomonas*, *Alcaligenes*, and *Polaromonas* strains) and GP (292 bp; *Rhodococcus*, *Mycobacterium*, *Nocardioides*, and *Terrabacter* strains) PAH bacterial degraders (Cébron et al. 2008). We compared the T-RFLP fingerprints digested with MspI of bacterial communities in soils after different biochars were added with those of the control microcosms (non-sterilized soil without biochar). Figure 6 shows the T-RFLP profiles of the samples with different biochars. Each peak on the profile corresponded to anonymous taxa referred to as an OTU, and the peak area corresponded to the proportion of this OTU in the bacterial community. Such a peak may be complex and may correspond to several bacterial species. Regardless of their anonymity and complexity, the T-RFLP profiles provided a convenient integrated method to detect the changes in microbial communities. The results showed that the bacterial communities contained a specific proportion of peaks common to all samples. However, samples differed in the profiles of bacterial communities, and a larger peak area was observed in the samples from soils receiving biochar.

Figure 6 shows the comparison of bacterial community structure in soil with biochar and those of the control microcosms. Base pair (bp) fragments 10, 11, and 13 with abundance >4 % were detected as major peaks. This finding indicated that these fragments were dominant populations. The T-RFs of 9, 14, and 156 bp were detected in biochar treatment but not in the control sample. The abundance of 9 and 14 bp was 18.48 and 5.16 % in RH350, respectively. The abundance of 9, 98, 99, and 156 bp was not detected in DM350; 8 bp (8.81 %) was detected, but 9 bp did not appear in RH500. These results showed significant changes in terms of GP PAH degradation bacterial community structure between the biochar treatment groups and the control group.

4 Conclusions

The present study showed that the average removal efficiencies of two-ring to four-ring PAHs in non-sterilized soil with biochar increased by 35 to 37 % compared with those in sterilized soil. Molecular biology analysis results demonstrated that biochar amendment can stimulate PAH-metabolizing bacterial activity by enhancing the number of 16S rDNA, *nir*S, and PAH-RHDα gene copies in PAH-contaminated soil. RH350 most effectively stimulated PAH dissipation in contaminated soil. Further studies should be conducted to evaluate the effect of biochar on PAH biodegradation in different soils and application rate of biochar.

References

Ambrosoli R, Petruzzelli L, Minati JL, Marsan FA (2005) Anaerobic PAH degradation in soil by a mixed bacterial consortium under denitrifying conditions. Chemosphere 60:1231–1236

American Society for Testing and Materials (ASTM) (2000) Annual Book of ASTM Standards, Soil and Rock. West Conshohocken, PA: American Society for Testing and Materials.

Baldock JA, Smernik RJ (2002) Chemical composition and bioavailability of thermally altered *Pinus resinosa* (red pine) wood. Org Geochem 33:1093–1109

Brewer CE, Schmidt-Rohr K, Satrio JA, Brown RC (2009) Characterization of biochar from fast pyrolysis and gasification systems. Environ Prog Sust Energy 28:386–396

Cantrell KB, Martin JH 2nd (2012) Stochastic state-space temperature regulation of biochar production. Part II: application to manure processing via pyrolysis. J Sci Food Agric 92:490–495

Cébron A, Norini MP, Beguiristain T, Leyval C (2008) Real-Time PCR quantification of PAH-ring hydroxylating dioxygenase (PAH-RHD alpha) genes from gram positive and gram negative bacteria in soil and sediment samples. J Microbiol Methods 73:148–159

Cébron A, Beguiristain T, Faure P, Norini MP, Masfaraud JF, Leyval C (2009) Influence of vegetation on the in situ bacterial community and polycyclic aromatic hydrocarbon (PAH) degraders in aged PAH-contaminated or thermal-desorption treated soil. Appl Environ Microbiol 75:6322–6330

Cerniglia CE (1993) Biodegradation of polycyclic aromatic hydrocarbons. Curr Opin Biotechnol 3:351–368

Chen B, Yuan M, Qian L (2012) Enhanced bioremediation of PAH-contaminated soil by immobilized bacteria with plant residue and biochar as carriers. J Soils Sediments 12:1350–1359

Cheng CH, Lehmann J, Thies JE, Burton SD, Engelhard MH (2006) Oxidation of black carbon by biotic and abiotic processes. Org Geochem 37:1477–1488

Colombo M, Cavalca L, Bernasconi S, Andreoni V (2011) Bioremediation of polyaromatic hydrocarbon contaminated soils by native microflora and bioaugmentation with *Sphingobium*

chlorophenolicum strain C3R: a feasibility study in solid- and slurry-phase microcosms. Int Biodeterior Biodegrad 65:191–197

Dean-Ross D, Moody J, Cerniglia CE (2002) Utilisation of mixtures of polycyclic aromatic hydrocarbons by bacteria isolated from contaminated sediment. FEMS Microbiol Ecol 41:1–7

Environmental Protection Agency (USEPA) (1986) Test methods for evaluating solid waste. Laboratory Manual Physical/Chemical Methods. U.S. Gov. Print Office, Washington, DC

European Union, Commission Recommendation 2005/108/EC (2005) Off J Eur Commun Law 34:43

Fredslund L, Sniegowski K, Wick LY, Jacobsen CS, De Mot R, Springael D (2008) Surface motility of polycyclic aromatic hydrocarbon (PAH)-degrading mycobacteria. Res Microbiol 159:255–262

Guo GX, Deng H, Qiao M, Mu YJ, Zhu YG (2011) Effect of pyrene on denitrification activity and abundance and composition of denitrifying community in an agricultural soil. Environ Pollut 159:1886–1895

Habe H, Omori T (2003) Genetics of polycyclic aromatic hydrocarbon metabolism in diverse aerobic bacteria. Biosci Biotechnol Biochem 67:225–243

Hale SE, Hanley K, Lehmann J, Zimmerman AR, Cornelissen G (2011) Effects of chemical, biological, and physical aging as well as soil addition on the sorption of pyrene to activated carbon and biochar. Environ Sci Technol 45:10445–10453

Haritash AK, Kaushik CP (2009) Biodegradation aspects of polycyclic aromatic hydrocarbons (PAHs): a review. J Hazard Mater 169:1–15

Hgberg MN, Hgberg P, Myrold DD (2007) Is microbial community composition in boreal forest soils determined by pH, C-to-N ratio, the trees, or all three? Oecologia 150:590–601

Hilber I, Blum F, Leifeld J, Schmidt HP, Bucheli TD (2012) Quantitative determination of PAHs in biochar: a prerequisite to ensure its quality and safe application. J Agric Food Chem 60:3042–3050

Jeffery S, Bezemer TM, Cornelissen G, Kuyper TW, Lehmann J, Mommer L, Sohi SP, van de Voorde TFJ, Wardle DA, Van Groenigen JW (2013) The way forward in biochar research: targeting trade-offs between the potential wins. GCB Bioenergy. doi:10.1111/gcbb.12132

Jurelevicius D, Alvarez VM, Peixoto R, Rosado AS, Seldin L (2012) Bacterial polycyclic aromatic hydrocarbon ring-hydroxylating dioxygenases (PAH-RHD) encoding genes in different soils from King George Bay, Antarctic Peninsula. Appl Soil Ecol 55:1–9

Karapanagioti HK, Gossard CM, Strevett KA, Kolar RL, Sabatini DA (2001) Model coupling intraparticle diffusion/sorption, nonlinear sorption, and biodegradation processes. J Contam Hydrol 48:1–21

Keiluweit M, Kleber M, Sparrow MA, Simoneit BR, Prahl FG (2012) Solvent-extractable polycyclic aromatic hydrocarbons in biochar: influence of pyrolysis temperature and feedstock. Environ Sci Technol 46:9333–9341

Keith LH, Telliard WA (1979) Priority pollutants I—a perspective view. Environ Sci Technol 13:416–423

Lehmann J, Rillig MC, Thies J, Masiello CA, Hockaday WC, Crowley D (2011) Biochar effects on soil biota—a review. Soil Biol Biochem 43:1812–1836

Lu XY, Li B, Zhang T, Fang H H (2012) Enhanced anoxic bioremediation of PAHs-contaminated sediment. Bioresour Technol 104:51–58

Meckenstock RU, Safinowski M, Griebler C (2004) Anaerobic degradation of polycyclic aromatic hydrocarbons. FEMS Microbiol Ecol 49:27–36

Meng L, Zhu YG (2010) Pyrene biodegradation in an industrial soil exposed to simulated rhizodeposition: how does it affect functional microbial abundance? Environ Sci Technol 45:1579–1585

Miller RH, Keeney DR (1982) Methods of soil analysis, part 2: chemical and microbiological properties, 2nd edn. American Society of Agronomy. Soil Science Society of America, Madison, WI. 9:539–577

Moody JD, Freeman JP, Doerge DR, Cerniglia CE (2001) Degradation of phenanthrene and anthracene by cell suspensions of *Mycobacterium* sp strain PYR-1. Appl Environ Microbiol 67:1476–1483

Peng RH, Xiong AS, Xue Y, Fu XY, Gao F, Zhao W, Tian YS, Yao QH (2008) Microbial biodegradation of polyaromatic hydrocarbons. FEMS Microbiol Rev 32:927–955

Pietikäinen J, Kiikkilä O, Fritze H (2000) Charcoal as a habitat for microbes and its effect on the microbial community of the underlying humus. Oikos 89:231–242

Qin G, Gong D, Fan MY (2013) Bioremediation of petroleum-contaminated soil by biostimulation amended with biochar. Int Biodeterior Biodegrad 85:150–155

Quilliam RS, Rangecroft S, Emmett BA (2013) Is biochar a source or sink for polycyclic aromatic hydrocarbon (PAH) compounds in agricultural soils? GCB Bioenergy 5:96–103

Rhodes AH, Carlin A, Semple KT (2008) Impact of black carbon in the extraction and mineralization of phenanthrene in soil. Environ Sci Technol 42:740–745

Schneegurt MA, Kulpa CF (1998) The application of molecular techniques in environmental biotechnology for monitoring microbial systems. Biotechnol Appl Biochem 27:73–79

Spokas KA, Cantrell KB, Novak JM, Archer DW, Ippolito JA, Collins HP, Boateng AA, Lima IM, Lamb MC, McAloon AJ, Lentz RD, Nichols KA (2012) Biochar: a synthesis of its agronomic impact beyond carbon sequestration. J Environ Qual 41:973–989

Steinbeiss S, Glexxner G, Antonietti M (2009) Effect of biochar amendment on soil carbon balance and soil microbial activity. Soil Biol Biochem 41:1301–1310

Uyttebroek M, Breugelmans P, Janssen M, Wattiau P, Joffe B, Karlson U, Ortega-Calvo JJ, Bastiaens L, Ryngaert A, Hausner M, Springael D (2006) Distribution of the *Mycobacterium* community and polycyclic aromatic hydrocarbons (PAHs) among different size fractions of a long term PAH-contaminated soil. Environ Microbiol 8:836–847

Vasilyeva GK, Strijakova ER, Nikolaeva SN, Lebedev AT, Shea PJ (2010) Dynamics of PCB removal and detoxification in historically contaminated soils amended with activated carbon. Environ Pollut 158:770–777

Wang T, Camps Arbestain M, Hedley M, Bishop P (2012) Chemical and bioassay characterisation of nitrogen availability in biochar produced from dairy manure and biosolids. Org Geochem 51:45–54

Williams PA, Fulop V, Garman EF, Saunders NFW, Ferguson SJ, Hajdu J (1997) Haem-ligand switching during catalysis in crystals of a nitrogen-cycle enzyme. Nature 389:406–412

Ye RW, Averill BA, Tiedje JM (1994) Denitrification: production and consumption of nitric oxide. Appl Environ Microbiol 60:1053–1058